

Article (refereed) - postprint

Kentisbeer, J.; Leeson, S.R.; Malcolm, H.M.; Leith, I.D.; Braban, C.F.; Cape, J.N. 2014. **Patterns and source analysis for atmospheric mercury at Auchencorth Moss, Scotland.** *Environmental Science: Processes & Impacts*, 16 (5). 1112-1123. [10.1039/c3em00700f](https://doi.org/10.1039/c3em00700f)

Copyright © The Royal Society of Chemistry 2014

This version available <http://nora.nerc.ac.uk/504958/>

NERC has developed NORA to enable users to access research outputs wholly or partially funded by NERC. Copyright and other rights for material on this site are retained by the rights owners. Users should read the terms and conditions of use of this material at <http://nora.nerc.ac.uk/policies.html#access>

This document is the author's final manuscript version of the journal article following the peer review process. Some differences between this and the publisher's version may remain. You are advised to consult the publisher's version if you wish to cite from this article.

<http://www.rsc.org>

Contact CEH NORA team at
noraceh@ceh.ac.uk

Patterns and source analysis for atmospheric mercury at Auchencorth Moss, Scotland

J. Kentisbeer*, S. R. Leeson, H. M. Malcolm, I. D. Leith, C.F. Braban and J.N. Cape

Centre for Ecology & Hydrology, Bush Estate, Penicuik, Midlothian, EH26 0QB

jkbeer@ceh.ac.uk

5 Abstract

Gaseous elemental (GEM), particulate bound (PBM) and gaseous oxidised (GOM) mercury species were monitored between 2009-2011 at the rural monitoring site, Auchencorth Moss, Scotland using the Tekran speciation monitoring system. GEM average for the three year period was $1.40 \pm 0.19 \text{ ng m}^{-3}$ which is comparable with other northern hemisphere studies. PBM and GOM concentrations are very low in 2009 and 2010 with geometric mean (x/÷ Standard Deviation) PBM values of 2.56 (x/÷ 3.44) and 0.03 (x/÷ 17.72) pg m^{-3} and geometric mean (x/÷ Standard Deviation) GOM values of 0.11 (x/÷ 4.94) and 0.09 (x/÷ 8.88) pg m^{-3} respectively. Using wind sector analysis and air mass back trajectories, the importance of local and regional sources on speciated mercury are investigated and we show the long range contribution to GEM from continental Europe, and that the lowest levels are associated with polar and marine air masses from the north west sector.

Key Words

Mercury, speciation, GEM, PBM, GOM

Introduction

20 Mercury enters the atmosphere from three sources: natural emissions, anthropogenic
emissions and reemission. Exact figures are uncertain but natural emissions are thought to
comprise about 10% of total emissions to the atmosphere annually and include releases
from volcanic eruptions, geothermal systems, erosion as well as evasion from the oceans.¹⁻⁵
About 30% are thought to be anthropogenic emissions from activities such as coal burning,
25 mining, smelting, cement production, oil refining, artisanal gold mining, chemical
manufacture and consumer waste.^{3, 6-8} The remaining 60% of emissions are thought to be
from re-emission of previously deposited mercury, mercury which has been deposited to
soils, vegetation or surface waters, that is subsequently returned to the atmosphere from
process such as evaporation from surface deposits, biomass burning or forest fires^{3, 9}.

30 Atmospheric mercury predominantly takes three forms: gaseous elemental mercury (GEM),
gaseous oxidised mercury (GOM) and particulate bound mercury (PBM). GEM makes up
>95% of total atmospheric mercury.^{10, 11} GEM is largely un-reactive and has low dry and wet
deposition rates¹² and therefore is a major vector for transport in the global mercury cycle.

Gaseous oxidised mercury (GOM) has an oxidation stage of +2 in inorganic molecules,¹³
35 being partly formed by reaction of GEM in the atmosphere with O₃ / OH / Br / BrO to form
species such as HgO, HgBr₂ Hg(OH)₂^{10, 11, 14}, with bromine chemistry likely to dominate¹⁵.

Mostly GOM is emitted directly to the atmosphere from point sources, where the mix of
compounds is more diverse depending on emission source. GOM species have a limited
atmospheric lifetime; most GOM species are readily removed by both wet and dry
40 deposition processes,^{12, 16, 17} leading to a short atmospheric lifetime, from a few hours to a
few weeks.^{10, 18} This depends on meteorology and atmospheric / emission plume

composition¹⁹, with a deposition footprint in the order of 10^2 - 10^3 km from the point source from which it was emitted. GOM is important for mercury cycling at the poles, where during polar sunrise large atmospheric mercury depletion events (AMDEs) occur due to rapid photochemical oxidation of GEM by halogen radicals to form GOM and ozone.²⁰⁻²² AMDEs resulting from oxidation by bromine have also been observed in the Dead Sea region²³ whilst AMDEs at Cape Point, South Africa are not bromine related.²⁴

PBM is formed from the adsorption of GEM or GOM on to particles, which can be emitted directly from point sources, or can form in the atmosphere²⁵ and has an atmospheric lifetime similar to GOM, with loss mechanisms of wet and dry deposition.^{12, 26, 27}

Mercury concentrations in the atmosphere increased dramatically during the 1800s due to gold rushes²⁸ across the globe and the industrial revolution before coming to a peak in the early 1980s and can be seen in glacier and lake sediment records.²⁹⁻³¹ Since then, the amount of observed atmospheric mercury has been gradually declining^{32, 33} through improvement on mercury emission controls and the current average GEM concentration in the northern hemisphere is between $1.4 - 1.7 \text{ ng m}^{-3}$.^{19, 32, 34-36}

Atmospheric mercury has become a more prominent interest with concerns about the effects of mercury on the health of both humans³⁷ and wildlife^{38, 39} ever since the diagnosis of Minamata disease in 1960⁴⁰. The highest risk to human health is thought to be through the consumption of fish with high levels of bioaccumulated methylmercury by higher predators.⁴¹⁻⁴³ The health risk is reflected in policy by the fact that many industrialised countries have issued fish consumption advisories, as well as the inclusion of mercury in the

United Nations Economic Commission for Europe (UNECE) convention on Long-Range Trans-boundary Air Pollution (LRTAP)¹³, with the European Air Framework 4th Daughter Directive requiring monitoring of mercury under the European Monitoring and Evaluation Programme (EMEP). 2013 also saw the signing of the UNEP Minamata Convention on Mercury, designed to protect human health and the environment from anthropogenic releases of mercury and its compounds to the environment.⁴⁴

In order to better understand the transport and fate of mercury in the atmosphere, speciated mercury concentrations have been measured in a variety of locations and scenarios⁴⁵⁻⁴⁷ however, few studies have been carried out in the UK.^{26, 48} One study (Gas phase mercury in the atmosphere of the United Kingdom, Lee et al, 1998) of Total Gaseous Mercury (TGM), comprising GEM and GOM, was carried out in 1995-6 at Harwell, a rural site in Oxfordshire, UK, which found a mean concentration of 1.68 ng m⁻³. This concentration is in line with other observed background concentrations in the northern hemisphere.^{19, 32, 34-36} The study by Lee et al (1998) assess the co-variation of TGM and SO₂, finding little correlation. However, wind sector analysis allowed them to identify probable sources as a lead-zinc smelter 50km to the west and an unidentified source to the east which they interpreted as 'generalised emissions from mainland northern Europe.' The study highlighted a diurnal pattern in TGM which they linked to surface emission fluxes of mercury at night under a stable nocturnal boundary layer.²⁶

In the north of the UK, speciated mercury measurements have been carried out over the period 2009 – 2011 at the UK EMEP Supersite, Auchencorth Moss. This extensive dataset can be used to investigate the drivers for mercury concentrations and the relationship with

85 long range transport and local sources. This paper will expand on the discussion in Kentisbeer et al (2011)⁴⁹ and will discuss in detail trends and patterns.

2. Materials and Methods

2.1 Site Description

90 Observations of atmospheric mercury were made between January 2009 and May 2010 (PBM) and September 2010 (GOM) December 2011 (GEM), at the Auchencorth Moss field site operated by the Centre for Ecology & Hydrology on behalf of the UK Government Department for Food and Rural Affairs (Defra). The site is in Midlothian, Scotland, ~20 km south-west of Edinburgh (55° 47' 32 N, 3° 14' 35 W). This is a rural, upland peat site, grazed by sheep and cattle with a uniform fetch comprising heathers, mosses and grasses in a remote location previously described in Flechard and Fowler, Drewer et al and Dinsmore et al.⁵⁰⁻⁵²

2.2 Mercury Analyser

100 Measurements of GEM, GOM and PBM were made using a mercury speciation system (Tekran, 2537A, 1130 and 1135 modules respectively.) The inlet samples air at 10 lmin⁻¹. During 2009 and 2010 the inlet was at a height of 0.9 m above ground level. During early 2011 the speciation units and inlet were transferred to a purpose built scaffold and the inlet height was raised to 4m. The height increase should lower surface effects and allow a more representative atmospheric background to be measured. Sample line filters were present in the sample train after the speciated fraction collection and on the analyser itself, both sets were changed monthly. The denuder was changed monthly and the particulate trap was

105

changed quarterly. Both were regenerated as per Tekran Guidance and detailed elsewhere.⁵³

Air is sampled through an impactor with a 2.5µm particle cut off. Within the instrument to separate the mercury components the air flow passes through a potassium chloride coated quartz annular denuder, to which the GOM sticks, then through a regenerable particle filter to remove PBM. The air then travels along a heated line to the analyser. The GEM analytical module subsamples of 0.9 L min⁻¹ of the air flow. The module consists of an automated dual channel amalgamation system which uses cold vapour atomic fluorescence spectroscopy (CVAFS, 253.7nm) to detect GEM. A schematic of the set up can be found in Lindberg et al (2002.)⁵⁴

Using a resolution of 5 minutes, the dual channel system allows continuous sampling of ambient air and pre-concentration of mercury by adsorption on to one of the two gold cartridges, whilst the other cartridge is simultaneously desorbed and analysed. The system works on a two hour cycle, during hour one, GEM is analysed every 5 minutes, whilst PBM and GOM are collected. During hour two, PBM and GOM are analysed, meaning GEM is not sampled. It should be noted that the Tekran units all suffered from extended down time periods during the three years. Data captures for the period January 2009 – December 2011 for each species were: GEM (72%), PBM (31%) and GOM (47%).

Automatic calibration of the instrument occurred every 26 hours using an internal permeation source. Two point calibrations, a zero and a span are completed separately for each cartridge with the permeation source giving ~1 pg s⁻¹ @ 50°C. 111 pg of mercury are

injected by the permeation source during auto-calibration, giving an effective concentration of 24.667 ng m⁻³. This was supplemented by annual permeation source verification tests using the external calibration source (Tekran 2505). This process uses saturated mercury vapour injections of known amounts of mercury to bracket the permeation rate of the internal source and thus verify the emission rate and calibration accuracy.⁵⁵ The instrument is not specifically calibrated with PBM or GOM, as these are analysed as GEM after they are thermally desorped from the particulate trap and denuder respectively. This makes uncertainty in these measurements hard to quantify.

The manufacturer stated detection limit is <0.1 ng m⁻³.⁵⁶ The method detection limit (MDL) for both GOM and PBM is not well defined by the manufacturer. For this study we have used log-normal probability plots to estimate the effective limit of detection for these two species. In this method the log values of the data are plotted against the normal-probability (z), to create a log-normal probability plot⁵⁷. If the log-transformed data have a normal distribution, all of the data will fit on to a straight line, however, at the lower end, the point at which the data no longer fit on to a straight line of best fit can be said to be the effective limit of detection. At the higher end, excursion from the line of best fit can be attributed to the influence of local sources. For the dataset presented here, the effective limit of detection for PBM and GOM is 0.45 pg m⁻³. Figure 1 shows the plot for GOM, from which the LOD is most easily measured. Data for these species were above the detection limit for 14.1% and 8.3% of the PBM and GOM dataset respectively. These plots can also be used to determine the geometric mean and standard deviation, from the intercept and gradient of the line of best fit (see section 3.1.) In order to properly characterise the

mercury species at the site, the statistics, tables and plots in this paper use the whole
150 dataset including all below LOD values.

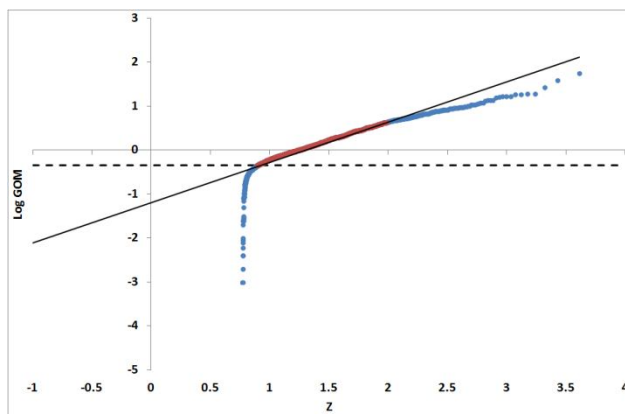


Figure 1: Plot of Log₁₀ of hourly GOM concentrations (pg m^{-3}) vs. The standard normal variate (z), showing the theoretical limit of detection for GOM. Gradient: 0.88 = Geometric Standard Deviation of $x/\div 7.6$, Intercept: -1.1 = Geometric Mean of 0.08 pg m^{-3} . The effective LOD is shown by the dashed line at $-0.35 = 0.45 \text{ pg m}^{-3}$ LOD.

155 Data presented here are hourly averages of the five minute resolution data. The one hour periods consist of twelve five minute measurements, but are not necessarily hour to hour, i.e. 12:00 - 13:00, they may be for example 12:20 – 13:20. Therefore, for the purposes of using air mass back trajectories and associating other met / pollutant data to the dataset, 160 the hour of the final five minute measurement in the period has been used, i.e. where the final five minute period was 14:35, then other associated data and back trajectories would be based on 14:00 hours.

2.4 Data analysis methods

Air mass back trajectories for Auchencorth Moss were calculated at three hour intervals using the NOAA HYSPLIT Trajectory Model (Hybrid Single Particle Lagrangian Integrated trajectory Model)⁵⁸ using the Global NOAA/NCAR reanalysis data archive. These 96 hour

back trajectories were run with a start height of 10 m above ground level, to best represent the sampling height. These trajectories were used as part of the OpenAir⁵⁹ package in the R statistical software⁶⁰ for analysis of the mercury data. The OpenAir package is an open source add on to the R package designed specifically for analysis of air pollution data and its development was funded by the UK Natural Environment Research Council (NERC), Kings College London, the UK Department for Food and Rural Affairs (Defra) and the University of Leeds.

3. Results and Discussion

3.1 Measurement overview

The time series of the measurements are shown in Figure 2 and Table 1 summarises the annual and seasonal average GEM, PBM and GOM values for Auchencorth Moss for 2009 – 2011. It can be seen that the annual average values for GEM are relatively consistent, with a three year mean (\pm Standard Deviation) of $1.40 \pm 0.19 \text{ ng m}^{-3}$. For PBM and GOM there is slightly more variation in the annual averages, with both species showing an approximate log-normal distribution. The best simple statistic to describe the distribution is the geometric mean and geometric standard deviation. Arithmetic and [geometric] mean PBM values of $3.71 \pm 5.19 [2.56 \times / \div 3.44]$ and $0.69 \pm 5.23 [0.03 \times / \div 17.72]$ pg m^{-3} and mean GOM values of $0.31 \pm 1.10 [0.11 \times / \div 4.94]$ and $0.57 \pm 2.26 [0.09 \times / \div 8.88]$ pg m^{-3} were observed in 2009 and 2010 respectively. The arithmetic and geometric means for GEM are very similar and are shown within seasons in Table 2 for comparison.

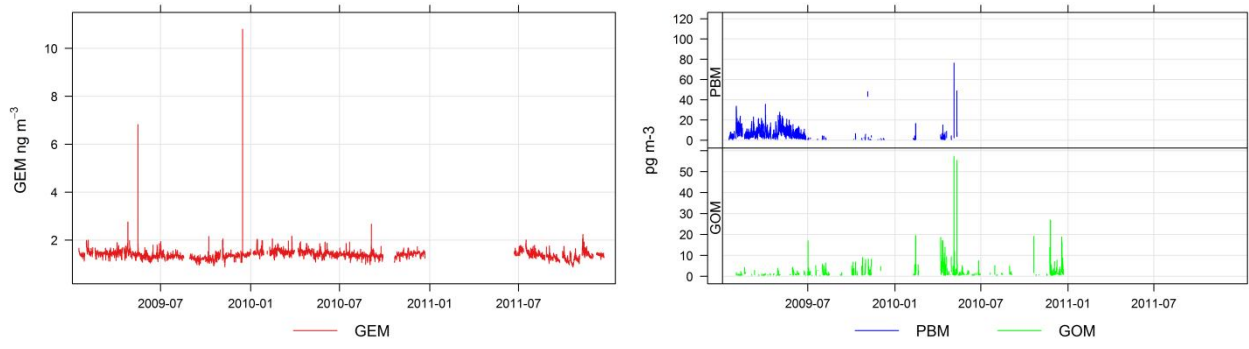


Figure 2: Time plots of hourly average a) GEM and b) PBM and GOM for 2009-2011 at Auchencorth Moss.

	Spring				Summer				Autumn				Winter				Total			
	Arithmetic Mean ± Standard Deviation	Geometric Mean x/± Geometric Standard Deviation	Median	90 th Percentile	Arithmetic Mean ± Standard Deviation	Geometric Mean x/± Geometric Standard Deviation	Median	90 th Percentile	Arithmetic Mean ± Standard Deviation	Geometric Mean x/± Geometric Standard Deviation	Median	90 th Percentile	Arithmetic Mean ± Standard Deviation	Geometric Mean x/± Geometric Standard Deviation	Median	90 th Percentile	Arithmetic Mean ± Standard Deviation	Geometric Mean x/± Geometric Standard Deviation	Median	90 th Percentile
2009																				
GEM	1.45 ± 0.21	1.44	1.44	1.59	1.33 ± 0.11	1.33	1.32	1.45	1.26 ± 0.13	1.26	1.25	1.39	1.43 ± 0.36	1.41	1.41	1.54	1.36 ± 0.23	-	1.35	1.52
PBM	8.33 ± 4.97	7.13 x/± 2.01	7.31	15.41	1.50 ± 2.48	1.36 x/± 2.65	0	4.98	0.26 ± 2.27	0.01 x/± 13.16	0	0.31	4.37 ± 5.66	3.04 x/± 2.87	2.77	11.62	3.71 ± 5.19	2.56 x/± 3.44	1.24	10.98
GOM	0.17 ± 0.46	0.12 x/± 3.75	0	0.62	0.47 ± 1.12	0.16 x/± 6.15	0	1.73	0.41 ± 1.70	0.09 x/± 7.42	0	1.06	0.17 ± 0.58	0.13 x/± 3.20	0	0.56	0.31 ± 1.10	0.11 x/± 4.94	0	0.89
2010																				
GEM	1.49 ± 0.12	1.48	1.49	1.60	1.39 ± 0.10	1.39	1.39	1.50	1.38 ± 0.13	1.37	1.38	1.50	1.51 ± 0.14	1.50	1.48	1.67	1.45 ± 0.13	-	1.44	1.58
PBM	0.87 ± 4.56	0.73 x/± 3.00	0	2.34	*	*	*	*	*	*	*	*	0.47 ± 5.88	0.05 x/± 6.30	0	0.52	0.68 ± 5.23	0.03 x/± 17.72	0	1.07
GOM	1.38 ± 3.96	0.22 x/± 10.69	0	4.78	0.13 ± 0.51	0.10 x/± 3.92	0	0.43	0.27 ± 1.48	0.05 x/± 7.01	0	0.58	0.79 ± 2.08	0.22 x/± 6.32	0	2.59	0.57 ± 2.26	0.09 x/± 8.88	0	1.41
2011																				
GEM	*	*	*	*	1.45 ± 0.13	1.45	1.44	1.63	1.33 ± 0.21	1.31	1.30	1.58	1.39 ± 0.05	1.38	1.40	1.44	1.38 ± 0.18	-	1.37	1.58
PBM	*	*	*	*	*	*	*	*	*	*	*	*	*	*	*	*	*	*	*	*
GOM	*	*	*	*	*	*	*	*	*	*	*	*	*	*	*	*	*	*	*	*
Total GEM	1.47 ± 0.17	-	1.47	1.49	1.39 ± 0.12	-	1.37	1.60	1.32 ± 0.17	-	1.31	1.53	1.46 ± 0.25	-	1.43	1.60	1.40 ± 0.19	-	0	1.57
Total PBM	6.02 ± 5.95	0.19 x/± 2.04	0	0.31	1.50 ± 2.48	1.36 x/± 2.65	4.95	13.86	0.26 ± 2.27	0.01 x/± 13.16	0	4.98	2.87 ± 6.05	1.83 x/± 3.24	0	8.62	3.11 ± 5.34	1.99 x/± 3.62	0	9.78
Total GOM	0.65 ± 2.60	0.09 x/± 9.33	0	0.86	0.29 ± 0.86	0.12 x/± 5.01	0	1.60	0.34 ± 1.60	0.06 x/± 7.72	0	0.94	0.48 ± 1.56	0.09 x/± 7.69	0	1.24	0.43 ± 1.76	0.08 x/± 7.63	0	1.09

Table 1: Annual and seasonal averages GEM (ng m⁻³) (arithmetic mean ± standard deviation, median and 90th percentile), PBM and GOM (both pg m⁻³) (arithmetic mean ± standard deviation, geometric mean x/± geometric standard deviation, median and 90th percentile) values for Auchencorth Moss. A * denotes periods of missing data due to instrument downtime, particularly affecting speciated measurements during 2011

190 The level of GEM observed at this background site is consistent with levels of GEM or TGM
observed in similar studies at rural locations, of between 1.3 – 1.7 ngm⁻³ (Table 2 and
references therein). This would be consistent with estimates of the northern hemispherical
background concentration. The 2009 GEM mean of 1.36 ± 0.23 ng m⁻³ is in good agreement
with that seen at the long term monitoring site at Mace Head, Ireland, with a 1.65 ± 0.13 ng
195 m⁻³ average for the same period (based on mean of monthly averages presented in
Ebinghaus et al, 2011.)⁶¹ Auchencorth has a slightly lower average value for GEM than most
other monitoring sites and extremely low levels of PBM and GOM. However, Auchencorth
may not be directly comparable to other monitoring sites in Europe and the Americas, as
land-locked sites are more likely to be influenced by continental air masses, which are more
200 polluted in nature, especially with PBM and GOM.

Place	Dates	GEM	sd	TGM	sd	PBM	Sd	GOM	sd
Yorkville, GA, USA⁴⁵	2007-8	1.35	0.17			4.33	5.59	8.55	18.8
CAMNet²⁰	1995-05			1.58	0.17				
Salmon Falls Creek Reservoir, ID, USA³⁵	2005-06	1.57	0.6					6.8	12
Huntingdon Forest, NY, USA⁴⁶	2007-09	1.3	0.4			4.1	7.8	1.3	3.3
Dexter, MI, USA	2004	1.59	0.59			6.1	5.51	3.8	6.62
Harwell, UK²⁶	1995-96			1.68					
Lista, Norway⁶²	1995-02			1.79					
Mace Head, Ireland⁶³	1995-02			1.75					
Mace Head, Ireland⁶¹	1996 -09*			1.65	0.13				
Zingst, Germany⁶⁴	1998-04			1.66					
St Ancient, Quebec, Canada³⁶	2005	1.65	0.42						
Waldhof, Germany⁶⁵	2009-11	1.61				6.3		1.0	

Table 2: GEM and TGM concentrations from other atmospheric mercury monitoring studies at locations in the northern hemisphere.

*Average and standard deviation based on mean of monthly averages presented in Ebinghaus et al, 2011.

3.2 Temporal Patterns in mercury concentrations

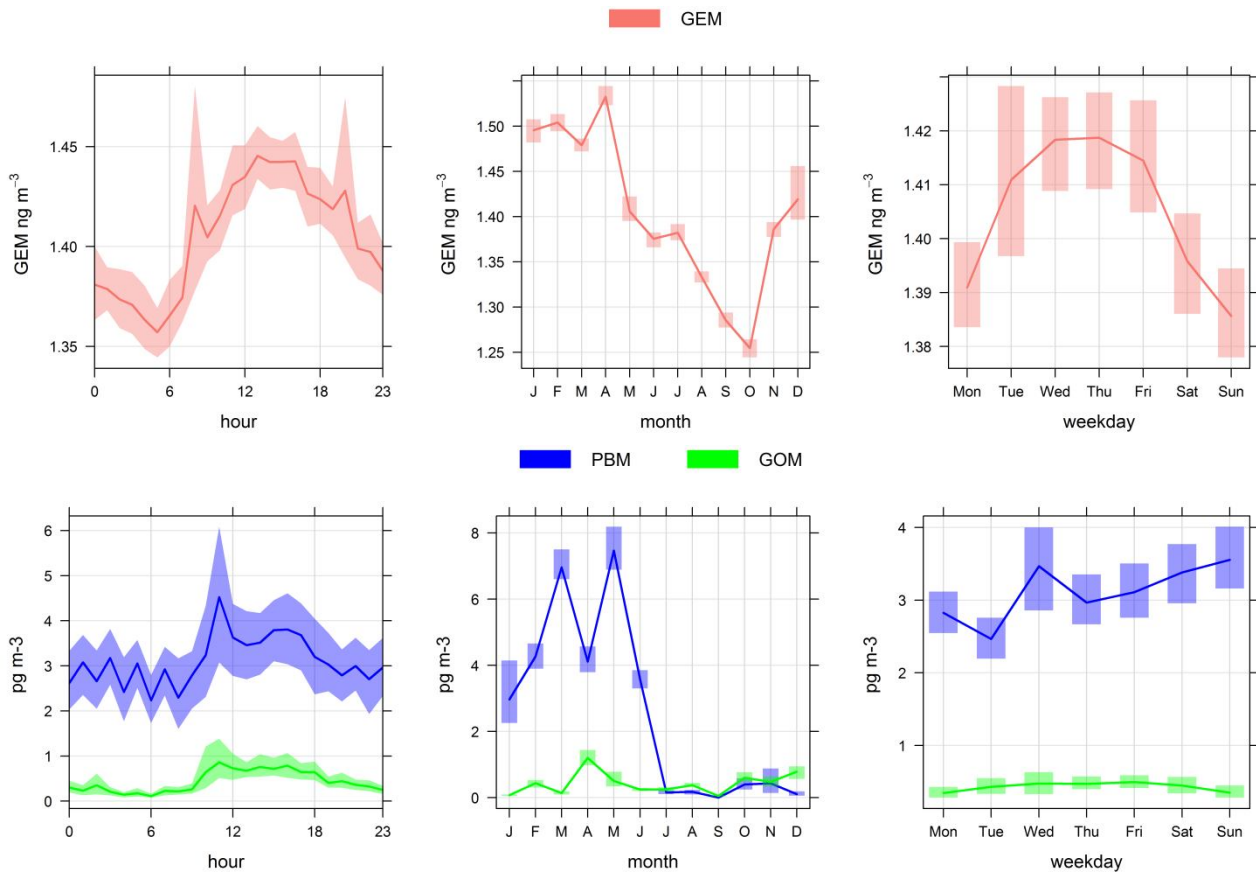


Figure 3: Time variation plots for 2009 data showing GEM (top), PBM and GOM (bottom) showing (from left to right), diurnal cycle, seasonal cycle and weekday trends for 0.9m inlet height data. The shaded areas are the 95% confidence intervals in the mean. Plots created using OpenAir in R.

Figure 3 shows time variation plots for the three mercury species; the solid lines represent the average of the data and the shaded areas are the 95% confidence intervals in the mean. (These plots were generated using OpenAir, a package for analysing atmospheric pollutant time series data sets in R⁵⁹.) As there is not enough data to properly discern any statistically significant difference between the sample heights, we have looked only at the data from

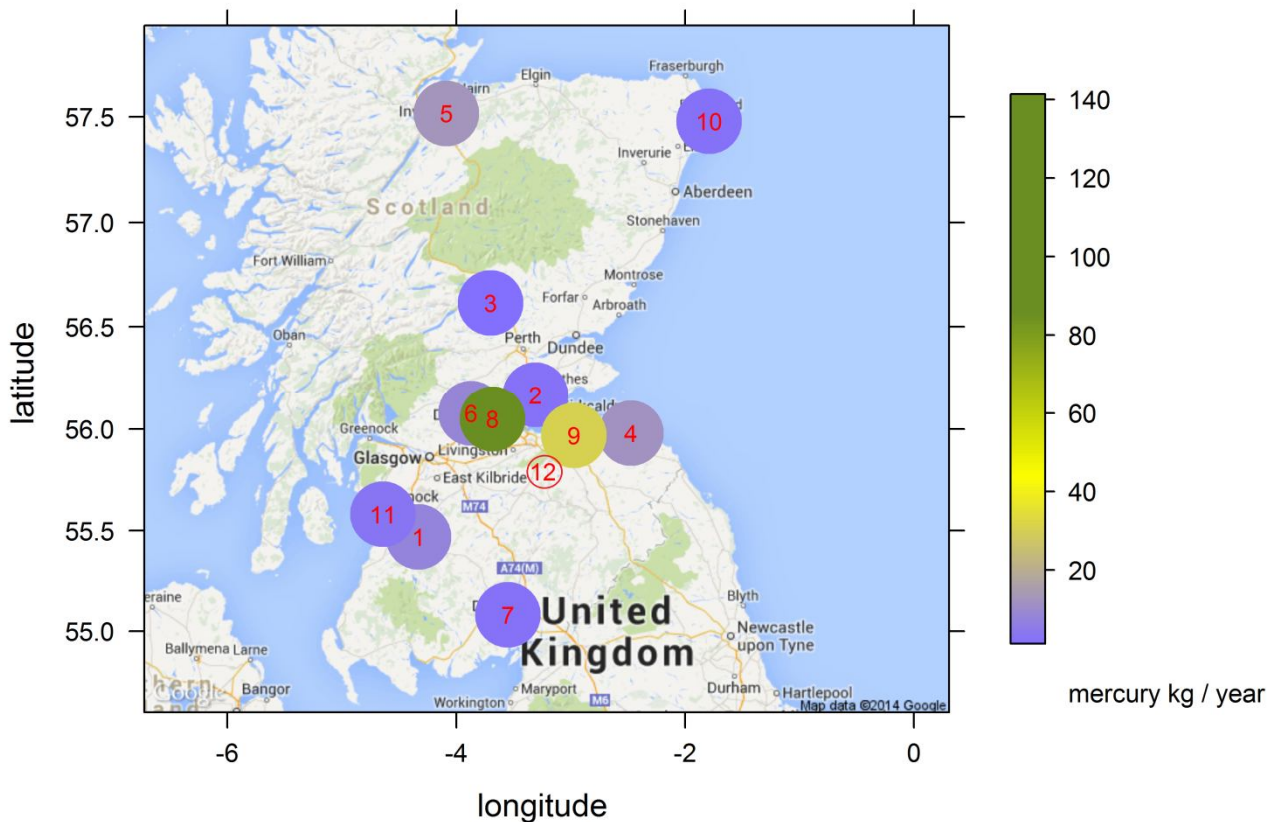
215 the 0.9m sample height (2009), so for GEM we can see that a diurnal cycle is present in the
data, with a minimum at around 6am and a maximum at around 1pm. This is consistent
with observed diurnal cycles in other studies^{35, 45, 65, 67, 68} and is most likely the result of
deposition below a nocturnal boundary layer, leading to an increase at dawn from re-
emission of mercury to the atmosphere from surfaces, influenced by increased convection
220 and mixing, through temperature and solar radiation, which has the same diurnal pattern
(not shown). The difference between maxima and minima is only slight (Figure 3), with an
absolute difference in averages of 0.08 ng m^{-3} , representing a 5.5% decrease from maxima
to minima. On a weekly scale, averages during the week are higher than at weekends;
however the difference between averages is only in the range of 0.03 ng m^{-3} and is not
225 statistically significant. The seasonal pattern for entire GEM dataset shows highest levels
during the winter and spring, with lower levels in the summer and autumn, which is
consistent with other studies.^{61, 65, 69} The reason for this pattern is not well understood but
could include meteorological conditions, higher emissions of GEM during winter and spring
from fossil fuel burning, or reduced GEM levels during the summer months due to greater
230 photochemical oxidation to GOM.

For PBM and GOM, there is less evidence of strong temporal patterns. For PBM there is a
small diurnal cycle between 7am and 6pm with a maximum at 11am; levels remain elevated
for much of the afternoon coinciding with the working day. There is no distinct weekly
235 pattern and the seasonal pattern is dominated by higher levels during the early half of 2009
however this is such a small dataset it cannot be assessed as to whether this is

representative for the site. The GOM dataset has a weak diurnal cycle, peaking in the late morning before falling away during the evening. It is hypothesised that the low concentrations are due to its remote location, distance from any significant industrial sources and high levels of wet deposition.²⁷

3.3 Spatial Patterns

In order to understand what sources might be influencing concentrations of mercury observed at Auchencorth Moss we have looked at the Scottish Pollutant Release Inventory provided by SEPA for mercury releases between 2009 and 2011.⁷⁰ Figure 4 shows that the largest emitters were Longannet (8) coal fired power stations in Fife and Cockenzie (9) coal fire power station in East Lothian, (Auchencorth Moss is number 12, red circle). Plots of the mercury species as a function of wind speed and direction can be seen in Figure 6



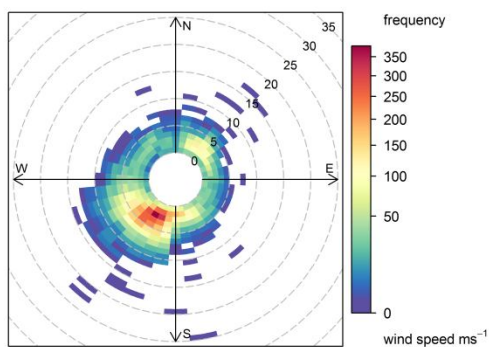
Site	Name	Operation
1	Egger (Barony) Limited	Timber Manufacture
2	EPR Scotland Limited	Biomass Plant
3	INEOS Manufacturing Scotland Ltd.	Petrochemicals
4	Lafarge Cement UK Limited	Cement Manufacture
5	Norbord Limited	Timber Product Manufacture
6	Norbord Limited	Timber Product Manufacture
7	Scotgen (Dumfries) Ltd	Energy From Waste
8	Scottish Power Generation Ltd	Coal Fired Power Station
9	Scottish Power Plc	Coal Fired Power Station
10	SSE Generation Limited	Gas Fired Power Station
11	UPM-Kymmene (UK) Limited	Paper Mill

12	Auchencorth Moss	Atmospheric Monitoring
----	------------------	------------------------

250

Figure 4: Point sources for average mercury emissions in kg year^{-1} for 2009-2011 in Scotland, Scottish Environmental Protection Agency (SEPA), Scottish Pollutant Release Inventory. (Map courtesy of Google Inc.)

A polar frequency plot of wind direction can be seen in Figure 5.



255

Figure 5: Polar frequency plot of wind speed (ms^{-1}) and direction at Auchencorth Moss. Plots created using OpenAir in R.

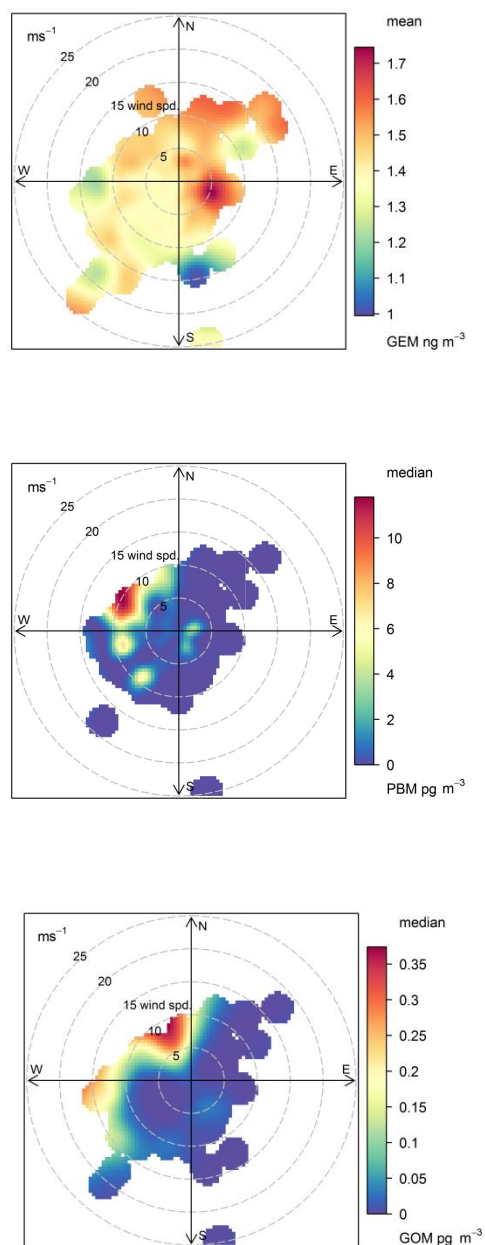


Figure 6: Polar Plots for (Top to bottom) a) GEM (mean), b) PBM (median) and c) GOM (Median) for 2009-2011 showing variation in species concentration by wind speed (ms^{-1}) and direction.. Plots created using OpenAir in R.

Figure 6a shows the variation of GEM concentration as a function of wind speed and direction and GEM. Concentrations of GEM are higher when winds are from the east and north-east and lower with winds from the south and south-west. The higher concentrations to the north-east are likely to be the influence of urban locations, such as the town of Penicuik and Edinburgh, as well as the power station at Cockenzie in East Lothian, whilst the

higher levels to the east could possibly be attributed to air mass arrivals from continental Europe⁴⁹ or activity close to the site (see below).

Figure 6b shows the same plot for PBM, this time plotted using median values to minimise the influence of extreme values. There are three small areas of elevated concentrations, one to the east and two to the south-west. The higher levels observed to the east are associated with relatively slow wind speeds of between 2 - 4 m s⁻¹, which could indicate a relatively local source or influence, whilst those to the south-west arrive on winds between 6 -10 m s⁻¹, indicating maybe that the sources of these emissions are slightly further away.

Close to the Auchencorth site are three peat extraction works, to the east, west and south-

west (Figure 7.) One hypothesis is that these peat extraction works are a possible source of

PBM. Soils with high organic matter content have been shown to have high concentrations of mercury (due to their low bulk density), built up over time and peat cores have been used to assess historic atmospheric mercury concentrations.³⁰ Hence, if the peat is

disturbed then it is possible that the mercury is re-suspended or emitted in the form of

PBM and GEM. Figure 8 shows a polar plot of the PBM : GEM ratio showing high ratios towards the peat extraction works, with the predominant source still to the north east.

Ottesen et al (2013) showed soil samples from the central belt of Scotland contained >0.1

mg kg⁻¹ of mercury relative to a European median of 0.03 mg kg⁻¹.⁷¹ Tipping et al (201)

showed similar levels of >0.163 mg kg⁻¹ for the area in which Auchencorth Moss is located.⁷²

Tipping et al also express soil mercury in terms of 'soil mercury pools', an expression of mass of metal per unit area. That study shows no correlation between peatlands and large mercury pools, however, it does show a pool >20 mg m⁻² for the Edinburgh, Lothians and

Fife region of Scotland, as well as industrial northern England and London. This indicates that peat extraction in general may not be a significant source of PBM and GOM, but in this locale, it may be. Peat extraction occurs when the weather is drier, with the machinery and peat drying operations generating significant quantities of dust; it could therefore be expected that summer months would generate the most dust and therefore we should see higher concentrations, however further investigation of this hypothesis is required using a larger dataset.



Figure 7: Map showing Auchencorth Moss (Yellow Pin) and the three peat extraction works to the east (1), west (2) and south west (3)

(Image courtesy of Google Maps.)

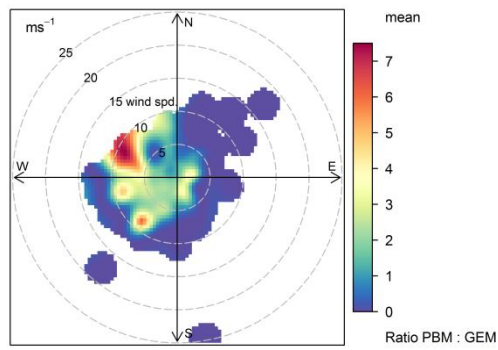


Figure 8: Polar plot for PBM / GEM ratio for 2009-2011, showing variation in mean ratio by wind speed (ms^{-1}) and direction. Plot created using OpenAir in R.

The largest concentrations are seen to the west-north-west on wind speeds greater than 5 m s^{-1} , indicating a source that is also some distance away. There are no distinct point sources from in this direction (Figure 5), but it is possible that this is the influence of the industrial and transport corridor of the Scottish central belt connecting Glasgow in the west and Edinburgh in the east.

Figure 6c shows the same plot for GOM, again using median values. This plot shows elevated concentrations of GOM at the Auchencorth site, with potential sources to the north-west and west. Highest levels are seen at wind speeds $> 5 \text{ ms}^{-1}$ indicating sources that are not immediately local. The higher concentrations to the west may be transport from industry near Glasgow, whilst the highest concentrations from the north-west are probably indicative of the Longannet coal-fired power station in Fife.

3.4 Air Mass Back Trajectories and Cluster Analysis

By using air mass back trajectories, we can look at where air masses that arrive at Auchencorth Moss have originated and what they might have passed over to arrive at the site. This process assigns the GEM concentrations observed at the site to the air masses

origin, which can allow us to create maps identifying patterns in concentrations by air mass origins. Figure 9 shows the concentration weighted trajectory (CWT, OpenAir) plot, which creates a concentration field from a grid domain to identify source areas of pollutants⁷³. This uses the concentration measured upon a trajectory's arrival at site and the residence time of that trajectory in each grid cell it passes through to create a mean concentration for each grid cell. When plotted as a map, this shows that air masses passing over which cells would, on average, give higher concentrations at the measurement site. Figure 9 shows that the Atlantic contribution to concentrations observed at Auchencorth is between 1.3 – 1.4 ng m⁻³, whilst higher observed concentrations in the order of 1.5 – 1.6 ng m⁻³ are strongly associated with Germany and continental Europe.

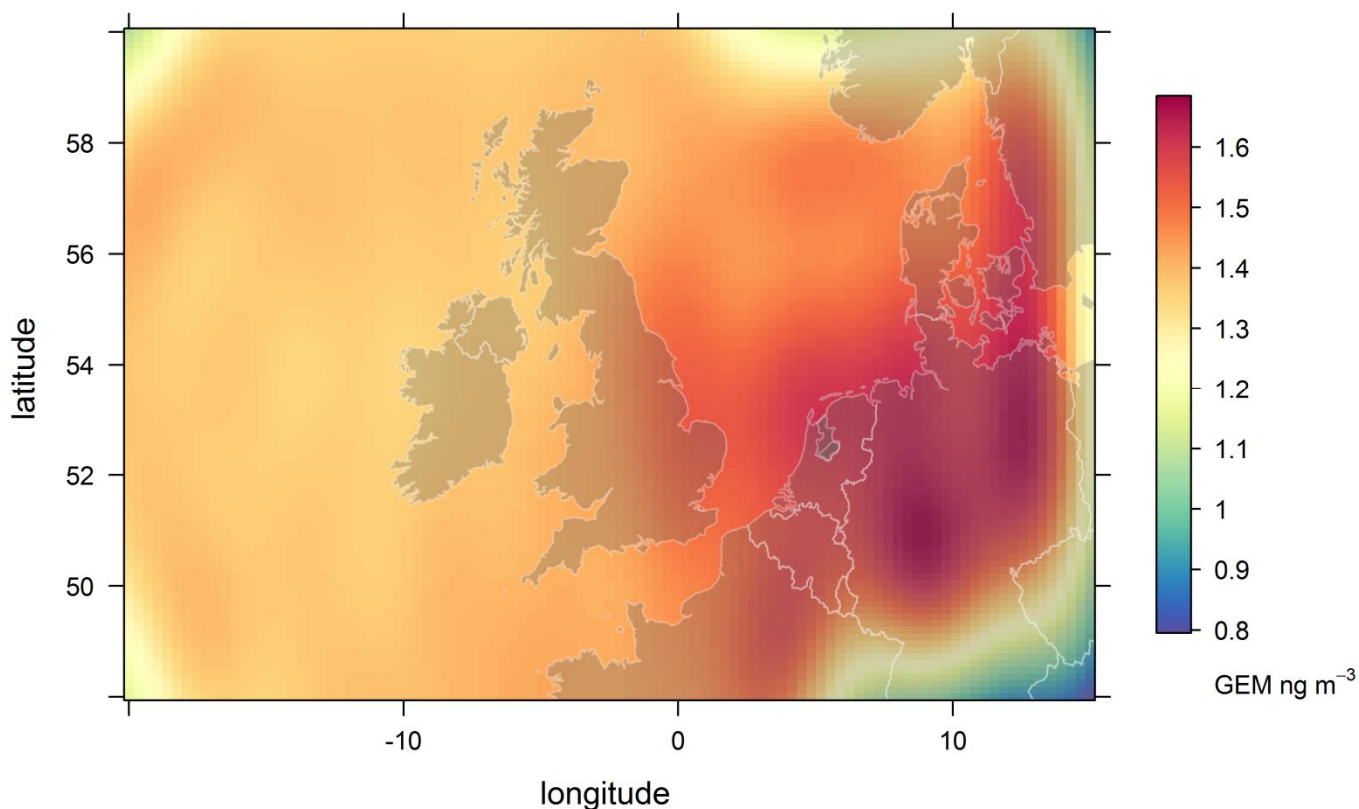


Figure 9: Concentration Weighted Trajectory (CWT) plot showing that higher GEM concentrations observed at Auchencorth Moss are strongly associated with air masses from Germany and continental Europe. Plot created using OpenAir in R.

By looking at cluster analysis of air mass back trajectories associated with GEM we are able to draw further conclusions about the sources and influences on the levels observed at Auchencorth Moss. By aggregating air masses arriving at the site for the full measurement period into 6 clusters (calculated using an angle-based distance matrix in OpenAir) with similar air mass origins, (Figure 10) and comparing the temporal characteristics of each cluster (Figure 11), it can be seen that cluster 6 is dominated by higher concentrations of GEM, originating from over continental Europe, whilst clusters 1, 3 and 4 have lower concentrations and originate from the north Atlantic ocean regions. Although GEM is not highly variable there are events with elevated and lower than average concentrations. Using a similar method as we used in Kentisbeer et al (2011), we have identified periods where GEM is greater than 3 standard deviations from the mean concentrations (68 values), and also trough values greater than two standard deviations below the mean (76 values). By again coupling these observed data with air masses, we can look at their origin in more detail. Figure 12 shows the individual air mass trajectories indicated by the dotted lines, showing the air mass origin and movements before it arrived at the site. Each trajectory is coloured according to the scale, showing the concentration of GEM observed at the time the air mass arrived on site. The majority of peak GEM concentrations originate from continental Europe and the lower concentrations arrive on cleaner air masses from the north Atlantic and Arctic regions.

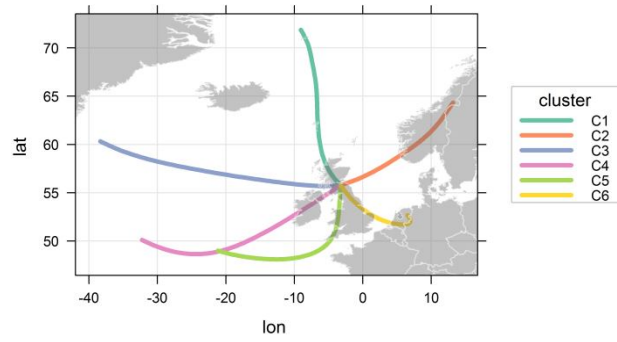
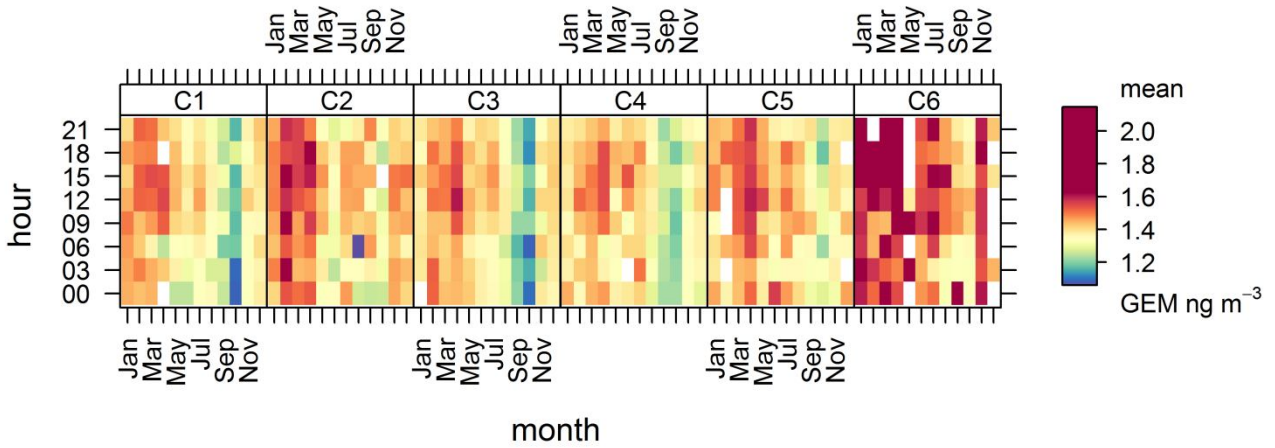


Figure 10: Cluster analysis of back trajectories arriving at Auchencorth Moss with air masses of similar origins into grouped into 6 average trajectory clusters.

350



Cluster	C1	C2	C3	C4	C5	C6
Trajectories in cluster	644	525	1252	1086	616	517

Figure 11: The temporal characteristics of GEM levels observed at Auchencorth Moss for each of the clusters, showing that cluster six is dominated by higher concentrations from continental Europe.

355

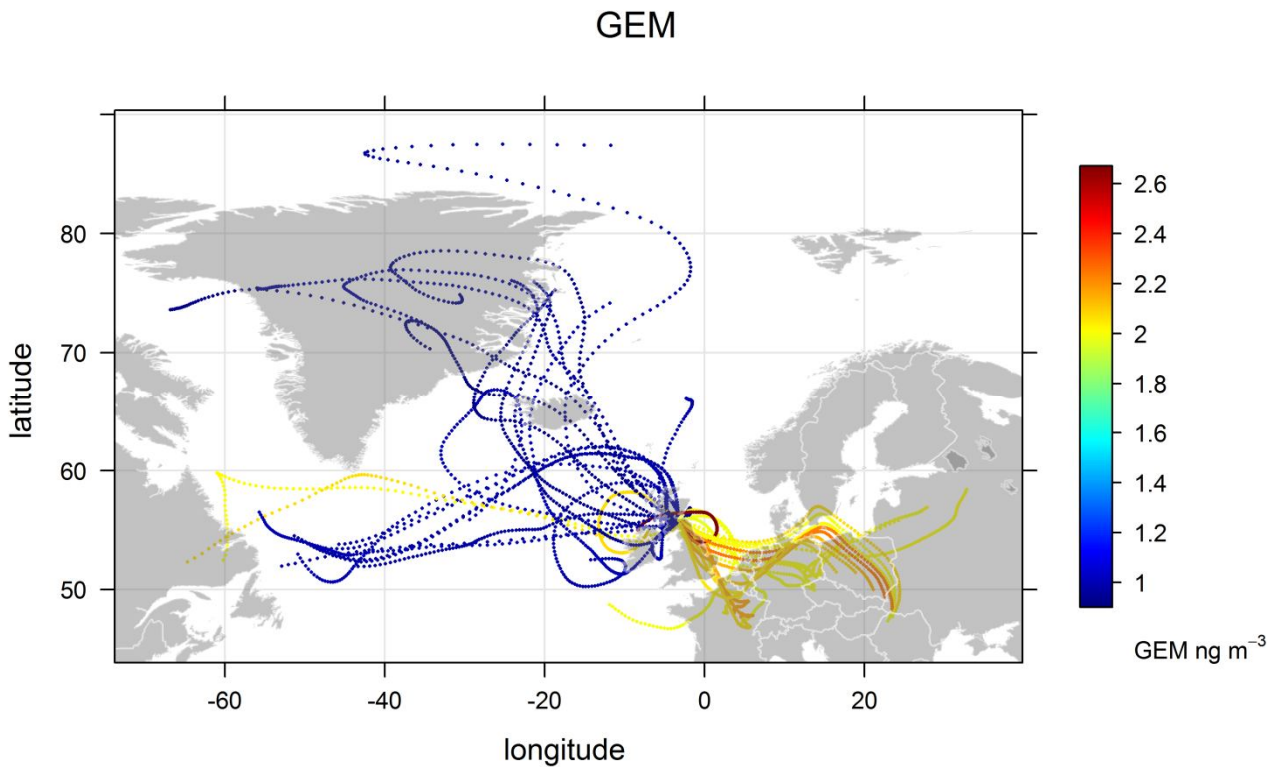


Figure 12: Individual air mass back trajectories for the highest (> 3 standard deviations from the mean) and lowest (> than 2 standard deviations from the mean) values of GEM arriving at Auchencorth Moss. Plots created using OpenAir in R.

4. Conclusions

The data presented here show that observed concentrations of gaseous elemental mercury at Auchencorth Moss are similar to other northern hemispherical background sites, with little to no influence from industrial point sources, but with a component of higher concentrations resulting from long range transport and the arrival of air masses from continental Europe. High concentrations arrive on air masses originating over Germany and eastern Europe, where heavy industry and therefore emission sources are more prevalent, whilst lower levels are observed arriving on air masses from the north Atlantic Ocean, a trend which is entirely independent of seasonal or other trends. These results are consistent with the declining south-east to north-west gradient in TGM observed in

Kentisbeer et al (2011), which used a network of 10 static samplers to assess the levels of
370 total gaseous mercury observed at 10 rural background locations across the UK.

Particulate mercury concentrations are higher at lower wind speeds indicating that local
sources are most significant for this site. The directional dependence of the data leads us to
believe that three peat extraction works could be some of the sources. Further work would
need to be undertaken to truly understand if this is the case.

375 GOM's diurnal cycle suggests that there may be some local formation through
photochemical processes. Whilst GOM is generally below detection limit to the south and
east, highest concentrations arrive on winds from the west and north-west indicating
sources influencing the site such as Glasgow to the west and Longannet coal-fired power
station to the north-west.

380 **Acknowledgements**

The data presented here were made under contract to the UK Department of the
Environment, Food and Rural Affairs (CPEA32). We gratefully acknowledge our colleagues in
CEH who operate and maintain the Auchencorth Moss field site.

1. D. A. Nimick, R. R. Caldwell, D. R. Skaar and T. M. Selch, *Sci Total Environ*, 2013, **443**, 40-54.
2. M. S. Gustin, *Applied Geochemistry*, 2008, **23**, 482-493.
3. UNEP, *Global Mercury Assessment 2013: Sources, Emissions, Releases and Environmental Transport*, UNEP Chemicals Branch, Geneva, Switzerland, 2013.
- 390 4. M. L. I. Witt, T. A. Mather, D. M. Pyle, A. Aiuppa, E. Bagnato and V. I. Tsanev, *Journal of Geophysical Research*, 2008, **113**.
5. J. Carrie, G. A. Stern, H. Sanei, R. W. Macdonald and F. Wang, *Applied Geochemistry*, 2012, **27**, 815-824.
6. N. Pirrone, S. Cinnirella, X. Feng, R. B. Finkelman, H. R. Friedli, J. Leaner, R. Mason, A. B. Mukherjee, G. B. Stracher, D. G. Streets and K. Telmer, *Atmospheric Chemistry and Physics*, 2010, **10**, 5951-5964.
- 395 7. D. Streets, J. Hao, Y. Wu, J. Jiang, M. Chan, H. Tian and X. Feng, *Atmospheric Environment*, 2005, **39**, 7789-7806.
8. E. G. Pacyna, J. M. Pacyna, K. Sundseth, J. Munthe, K. Kindbom, S. Wilson, F. Steenhuisen and P. Maxson, *Atmospheric Environment*, 2010, **44**, 2487-2499.
9. R. J. DiCOSTY, M. A. Callahan and J. A. Stanturf, *Water Air and Soil Pollution*, 2006, **176**, 77-91.
- 400 10. W. H. Schroeder and J. Munthe, *Atmospheric Environment*, 1998, **32**, 809-822.
11. S. E. Lindberg and W. J. Stratton, *Environmental Science & Technology*, 1998, **32**, 49-57.
12. X. Zhang, Z. Siddiqi, X. Song, K. L. Mandiwana, M. Yousaf and J. Lu, *Atmospheric Environment*, 2012, **50**, 60-65.
13. D. S. Lee, E. Nemitz, D. Fowler and R. D. Kingdon, *Atmospheric Environment*, 2001, **35**, 5455-5466.
- 405 14. X. B. Feng, J. Y. Lu, D. C. Gregoire, Y. J. Hao, C. M. Banic and W. H. Schroeder, *Analytical and Bioanalytical Chemistry*, 2004, **380**, 683-689.
15. C. D. Holmes, D. J. Jacob, E. S. Corbitt, J. Mao, X. Yang, R. Talbot and F. Slemr, *Atmospheric Chemistry and Physics*, 2010, **10**, 12037-12057.
16. M. Sakata and K. Marumoto, *Atmospheric Environment*, 2005, **39**, 3139-3146.
- 410 17. S. O. Lai, J. Y. Huang, P. K. Hopke and T. M. Holsen, *Science of the Total Environment*, **409**, 1320-1327.
18. L. M. Zhang, L. P. Wright and P. Blanchard, *Atmospheric Environment*, 2009, **43**, 5853-5864.
19. AMAP/UNEP, *Technical background Report for the Global Mercury Assessment 2013*, Arctic Monitoring and Assessment Programme, Oslo, Norway / UNEP Chemicals Branch, Geneva, Switzerland, 2013.
20. C. Temme, P. Blanchard, A. Steffen, C. Banic, S. Beauchamp, L. Poissant, R. Tordon and B. Wiens, *Atmos Environ*, 2007, **41**, 5423-5441.
- 415 21. A. Steffen, W. Schroeder, R. Macdonald, L. Poissant and A. Konoplev, *Science of the Total Environment*, 2005, **342**, 185-198.
22. P. A. Ariya, A. P. Dastoor, M. Amyot, W. H. Schroeder, L. Barrie, K. Anlauf, F. Raofie, A. Ryzhkov, D. Davignon, J. Lalonde and A. Steffen, *Tellus*, 2004, **56B**, 397 - 403.
- 420 23. E. Tas, D. Obrist, M. Peleg, V. Matveev, X. Fain, D. Asaf and M. Luria, *Atmospheric Chemistry and Physics*, 2012, **12**, 2429-2440.
24. E. G. Brunke, C. Labuschagne, R. Ebinghaus, H. H. Kock and F. Slemr, *Atmospheric Chemistry and Physics*, 2010, **10**, 1121-1131.
25. D. M. Feddersen, R. Talbot, H. Mao and B. C. Sive, *Atmospheric Chemistry and Physics*, 2012, **12**, 10899-10909.
- 425 26. D. S. Lee, G. J. Dollard and S. Pepler, *Atmospheric Environment*, 1998, **32**, 855-864.
27. A. P. Rowland, A. J. Lawlor, H. J. Guyatt and R. A. Wadsworth, *Journal of Environmental Monitoring*, 2010, **12**, 1747-1755.
28. L. D. Lacerda, *Water Air and Soil Pollution*, 1997, **97**, 209-221.
- 430 29. P. Schuster, D. P. Krabbenhoft, D. L. Naftz, L. D. Cecil, M. L. Olson, J. F. Dewild, D. D. Susong, J. R. Green and M. L. Abbot, *Environ. Sci. Technol.*, 2002, **36**, 2303 - 2310.
30. J. G. Farmer, P. Anderson, J. M. Cloy, M. C. Graham, A. B. MacKenzie and G. T. Cook, *Science of the Total Environment*, 2009, **407**, 5578-5588.
31. H. D. Yang, N. L. Rose, R. W. Battarbee and J. F. Boyle, *Environmental Science & Technology*, 2002, **36**, 1383-1388.
- 435 32. F. Slemr, E. G. Brunke, R. Ebinghaus and J. Kuss, *Atmospheric Chemistry and Physics*, 2011, **11**, 4779-4787.
33. A. L. Soerensen, D. J. Jacob, D. G. Streets, M. L. I. Witt, R. Ebinghaus, R. P. Mason, M. Andersson and E. M. Sunderland, *Geophys Res Lett*, 2012, **39**.

- 440 34. F. Sprovieri, N. Pirrone, R. Ebinghaus, H. Kock and A. Dommergue, *Atmospheric Chemistry and Physics*, 2010, **10**, 8245-8265.
35. M. L. Abbott, C.-L. Lin, P. Martian and J. Einerson, *Applied Geochemistry*, 2008, **23**, 438 - 453.
36. L. Poissant, M. Pilote, C. Beauvais, P. Constant and H. H. Zhang, *Atmospheric Environment*, 2005, **39**, 1275-1287.
37. P. Holmes, K. A. F. James and L. S. Levy, *Science of the Total Environment*, 2009, **408**, 171-182.
- 445 38. C. T. Driscoll, R. P. Mason, H. M. Chan, D. J. Jacob and N. Pirrone, *Environmental Science & Technology*, 2013, **47**, 4967-4983.
39. S. W. Tan, J. C. Meiller and K. R. Mahaffey, *Critical Reviews in Toxicology*, 2009, **39**, 228-269.
40. M. Harada, *Critical Reviews in Toxicology*, 1995, **25**, 1-24.
41. J. A. Davis, R. E. Looker, D. Yee, M. Marvin-Di Pasquale, J. L. Grenier, C. M. Austin, L. J. McKee, B. K. Greenfield, R. Brodberg and J. D. Blum, *Environ. Res.*, 2012, **119**, 3-26.
- 450 42. Y.-S. Hong, Y.-M. Kim and K.-E. Lee, *Journal of preventive medicine and public health = Yebang Uihakhoe chi*, 2012, **45**, 353-363.
43. A. M. Lando, S. B. Fein and C. J. Choiniere, *Environ. Res.*, 2012, **116**, 85-92.
44. UNEP, ed. U. N. E. Programme, Geneva, Switzerland, Editon edn., 2013.
- 455 45. U. S. Nair, Y. L. Wu, J. Walters, J. Jansen and E. S. Edgerton, *Atmospheric Environment*, 2012, **47**, 499-508.
46. H. D. Choi, J. Huang, S. Mondal and T. M. Holsen, *Sci Total Environ*, 2013, **448**, 96-106.
47. L. E. Gratz, G. J. Keeler, F. J. Marsik, J. A. Barres and J. T. Dvonch, *Sci Total Environ*, 2013, **448**, 84-95.
48. M. L. I. Witt, N. Meheran, T. A. Mather, J. C. M. de Hoog and D. M. Pyle, *Atmospheric Environment*, 2010, **44**, 1524-1538.
- 460 49. J. Kentisbeer, D. Leaver and J. N. Cape, *Journal of Environmental Monitoring*, 2011, **13**, 1653-1661.
50. C. R. Flechard and D. Fowler, *Q. J. R. Meteorol. Soc.*, 1998, **124**, 733-757.
51. J. Drewer, A. Lohila, M. Aurela, T. Laurila, K. Minkkinen, T. Penttila, K. J. Dinsmore, R. M. McKenzie, C. Helfter, C. Flechard, M. A. Sutton and U. M. Skiba, *Eur. J. Soil Sci.*, 2010, **61**, 640-650.
52. K. J. Dinsmore, U. M. Skiba, M. F. Billett, R. M. Rees and J. Drewer, *Soil Biol. Biochem.*, 2009, **41**, 1315-1323.
- 465 53. M. S. Landis, R. K. Stevens, F. Schaedlich and E. M. Prestbo, *Environ. Sci. Technol.*, 2002, **36**, 3000 - 3009.
54. S. E. Lindberg, S. Brooks, C.-J. Lin, K. J. Scott, M. S. Landis, R. K. Stevens, M. Goodsite and A. Richter, *Environ. Sci. Technol.*, 2002, **36**, 1245 - 1256.
55. Tekran, *Model 2537A Mercury Vapor Analyzer User Manual*, 2.21 edn., Toronto, Canada, 1999.
56. Tekran, *The Tekran Ambient Monitoring System: Continuous Ultra-Trace mercury Vapor Analysis*, 2009.
- 470 57. J. N. Cape, M. Coyle and P. Dumitrescu, *Atmospheric Environment*, 2012, **59**, 256-263.
58. R. R. Draxler and G. D. Rolph, *HYSPLIT (HYbrid Single-Particle Lagrangian Inetgrated Trajectory) Model*, <http://ready.arl.noaa.gov/HYSPLIT.php>, 2012.
59. D. C. Carslaw and K. Ropkins, *Environmental Modelling & Software*, 2012, **27-28**, 52-61.
60. R. C. Team, Foundation for Statistical Computing, Vienna, Austria, Editon edn., 2012.
- 475 61. R. Ebinghaus, S. G. Jennings, H. H. Kock, R. G. Derwent, A. J. Manning and T. G. Spain, *Atmospheric Environment*, 2011, **45**, 3475-3480.
62. I. Wängberg, J. Munthe, T. Berg, R. Ebinghaus, H. H. Kock, C. Temme, E. Bieber, T. G. Spain and A. Stolk, *Atmospheric Environment*, 2007, **41**, 2612-2619.
- 480 63. R. Ebinghaus, H. H. Kock, A. M. Coggins, T. G. Spain, S. G. Jennings and C. Temme, *Atmospheric Environment*, 2002, **36**, 5267-5276.
64. H. H. Kock, E. Bieber, R. Ebinghaus, T. G. Spain and B. Thees, *Atmospheric Environment*, 2005, **39**, 7549 - 7556.
65. A. Weigelt, C. Temme, E. Bieber, A. Schwerin, M. Schuetze, R. Ebinghaus and H. H. Kock, *Environ. Chem.*, 2013, **10**, 102-110.
- 485 66. D. A. Gay, D. Schmeltz, E. Prestbo, M. Olson, T. Sharac and R. Tordon, *Atmospheric Chemistry and Physics*, 2013, **13**, 11339-11349.
67. J. Stamenkovic, S. Lyman and M. S. Gustin, *Atmospheric Environment*, 2007, **41**, 6662-6672.
68. J. M. Sigler, H. Mao, B. C. Sive and R. Talbot, *Atmospheric Chemistry and Physics*, 2009, **9**, 4023-4030.
69. X. Lan, R. Talbot, M. Castro, K. Perry and W. Luke, *Atmospheric Chemistry and Physics*, 2012, **12**, 10569-10582.
- 490 70. S. E. P. A. (SEPA), *Scottish Pollutant Release Inventory (SPRI)*, http://www.sepa.org.uk/air/process_industry_regulation/pollutant_release_inventory.aspx, Accessed 20/05/2013, 2013.

495

71. R. T. Ottesen, M. Birke, T. E. Finne, M. Gosar, J. Locutura, C. Reimann and T. Tarvainen, *Applied Geochemistry*, 2013, **33**, 1-12.
72. E. Tipping, J. M. Poskitt, A. J. Lawlor, R. A. Wadsworth, D. A. Norris and J. R. Hall, *Environmental Pollution*, 2011, **159**, 3721-3729.
73. D. C. Carslaw, *The openair Project Newsletter - 14/02/2013*, 2013.

500